Supplement of Biogeosciences, 22, 305–321, 2025
https://doi.org/10.5194/bg-22-305-2025-supplement


Biogeosciences
Open Access

*Supplement of*

# Ensemble estimates of global wetland methane emissions over 2000–2020

**Zhen Zhang et al.**

*Correspondence to:* Zhen Zhang (yuisheng@gmail.com)

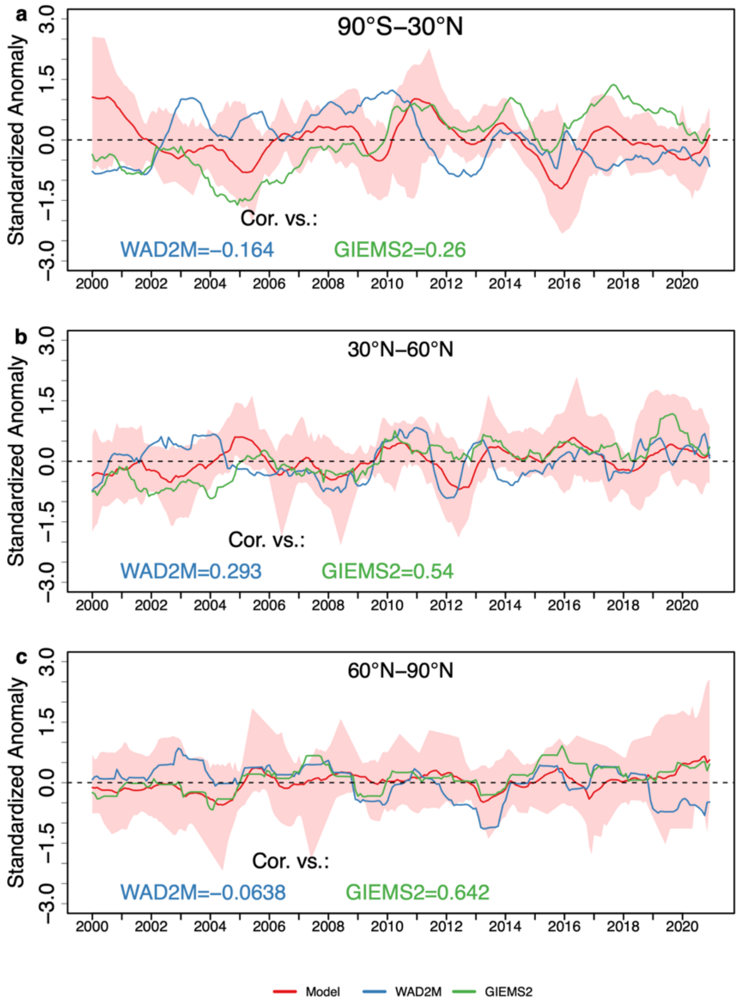


**Figure S1. Temporal variations in wetland anomalies in model ensemble in comparison with satellite-based products WAD2M and GIEMS2.** The wetland areal anomalies were calculated relative to the mean of 2000-2006 level and then standardized using a Z score. The shaded areas are the 1-standard deviation of model ensemble estimates. The solid lines are the 12-month running means of the anomalies. The correlations in the trend between model ensemble mean and satellite-based products are listed.

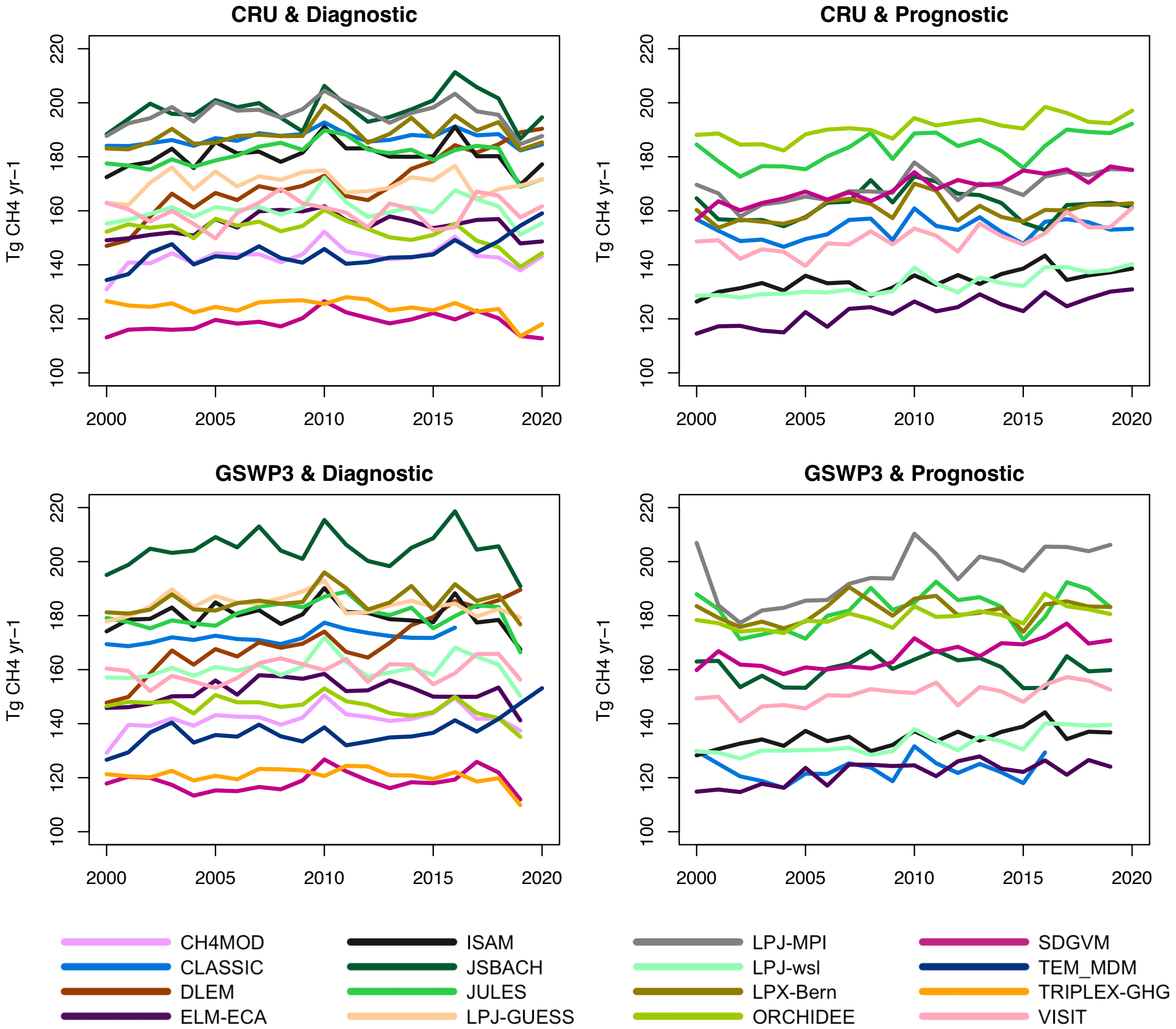


**Figure S2. Time series of annual total $CH_4$ emissions from the prognostic runs. Note that 11 of the 16 models have prognostic estimates.** Note that the diagnostic results are not used in interpreting temporal changes due to a discontinuity issue in a few tropical hotspots, which exists in some of the models (see Methods).

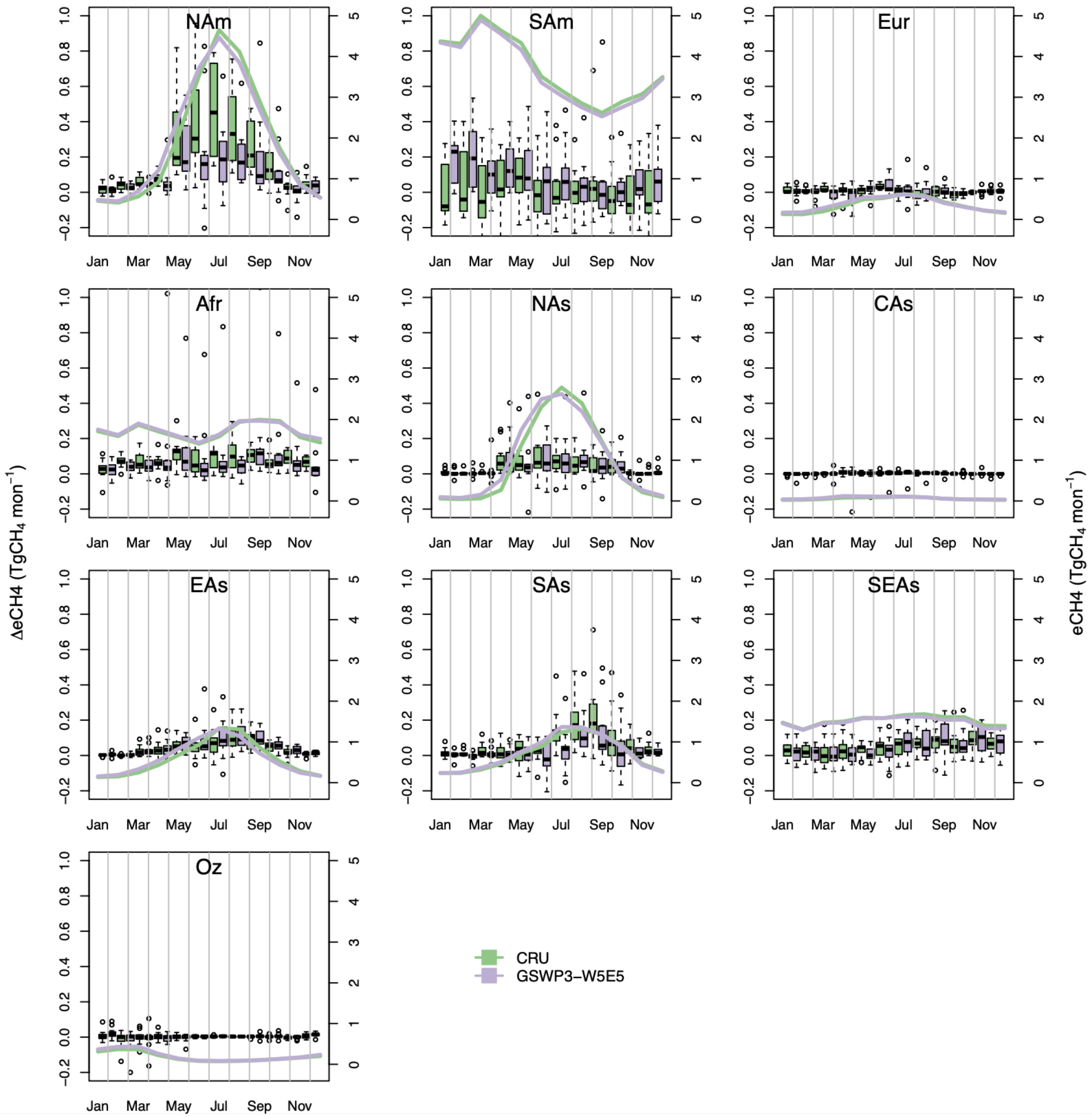

NAm
SAm
Eur
Afr
NAs
CAs
EAs
SAs
SEAs
Oz
Jan
Mar
May
Jul
Sep
Nov
ΔeCH4 (TgCH$_4$ mon$^{-1}$)
eCH4 (TgCH$_4$ mon$^{-1}$)
CRU
GSWP3-W5E5

**Figure S3. Regional changes in the seasonal cycle of $\Delta eCH_4$ and corresponding mean seasonal cycle.** The boxplots represent mean $\Delta eCH_4$ in the seasonal cycle during 2010-2019 relative to the average of 2000-2009. The black whiskers extend to the most extreme data points not considered outliers, which are denoted as dots. The colored lines represent the average seasonal cycle of 2000-2009 from the simulations grouped by two climate datasets, CRU and GSWP3-W5E5. Region Abbreviations: NAm, North America; SAm, South America; Eur, Europe; Afr, Africa; NAs, North Asia; CAs, Central Asia, EAs, East Asia; Sas, South Asia; SEAs, Southeast Asia; Oz, Oceania.

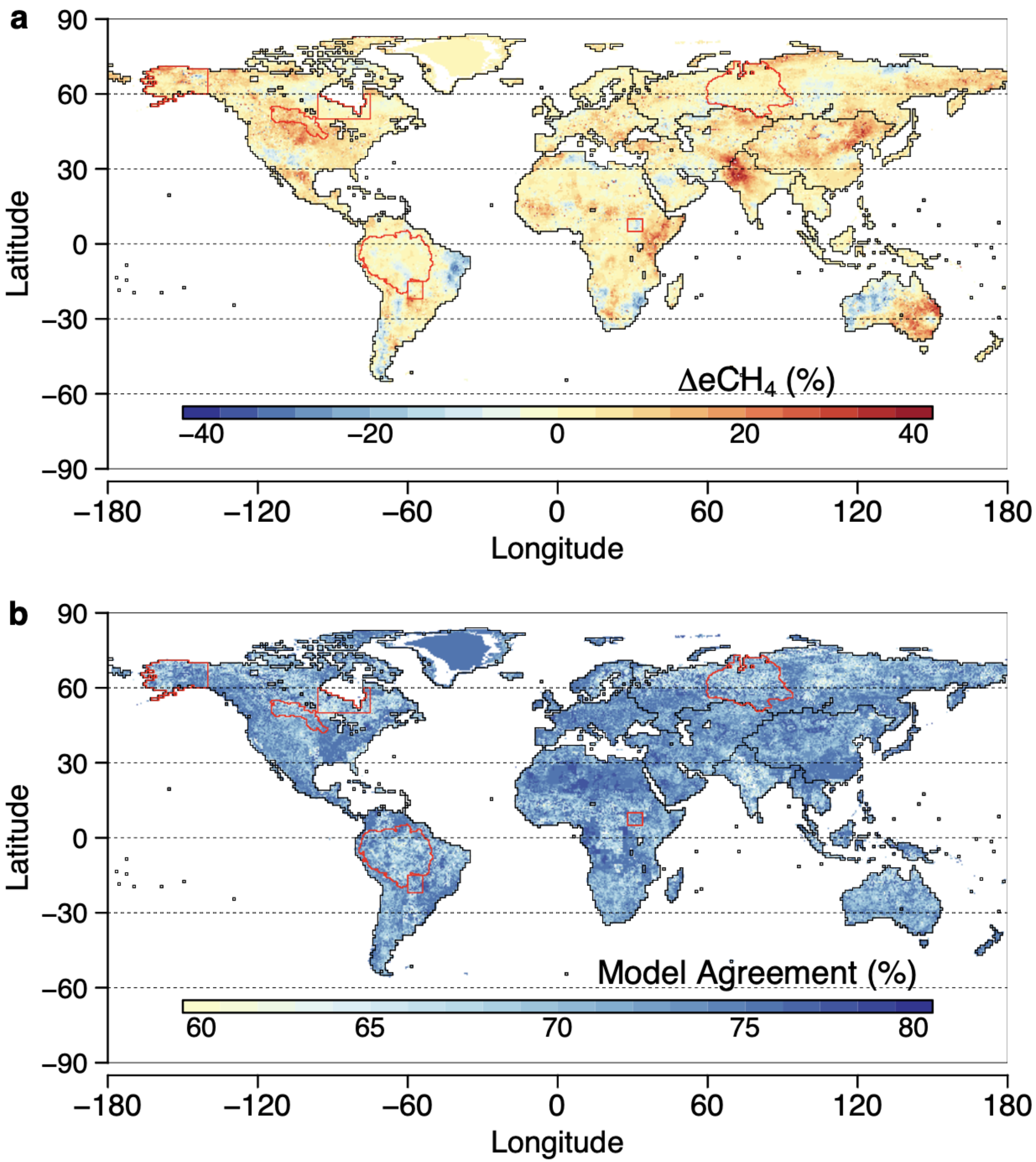
a
90
60
30
0
−30
−60
−90
Latitude
−180
−120
−60
0
60
120
180
Longitude
ΔeCH4 (%)
−40
−20
0
20
40
b
Model Agreement (%)
60
65
70
75
80

**Figure S4. Spatial distribution of $\Delta eCH_4$ in percentage between the 2010s and 2000s and the level of model agreement.** The level of model agreement (%) is defined as the ratio of the number of runs whose estimates fall within the 1-σ range of the whole ensemble to the number of total runs (n=22). The regional $CH_4$ hotspots in Table S3 are shown in red.

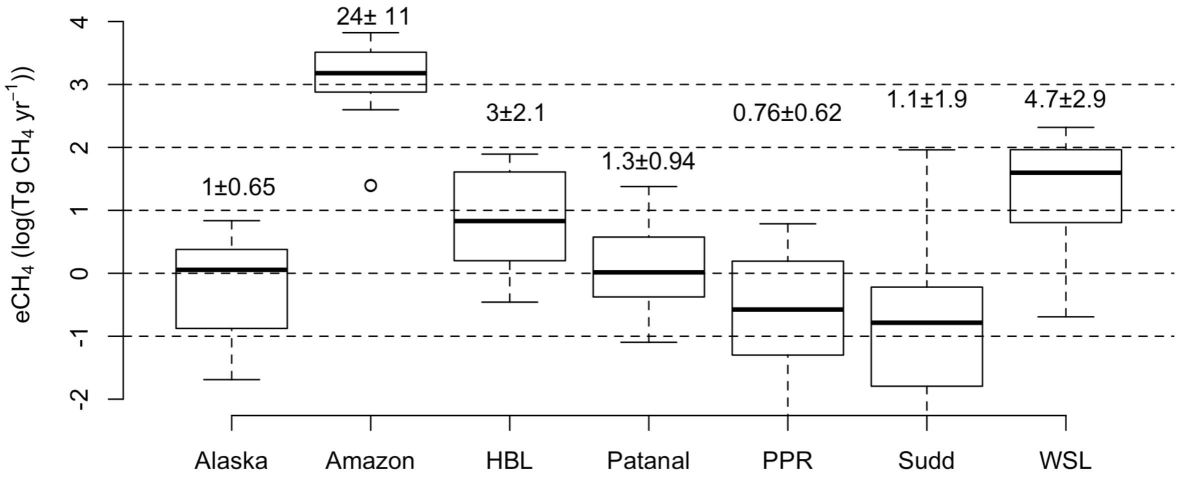


**Figure S5. Boxplot of mean $eCH_4$ for regional hotspots from the prognostic runs.** The model ensemble means are shown with one standard deviation for 2000-2020. The mask map is shown in Fig. S3. HBL, PPR, and WSL refer to 'Hudson Bay Lowland', 'Prairie Pothole Region', and 'West Siberian Lowland', respectively.

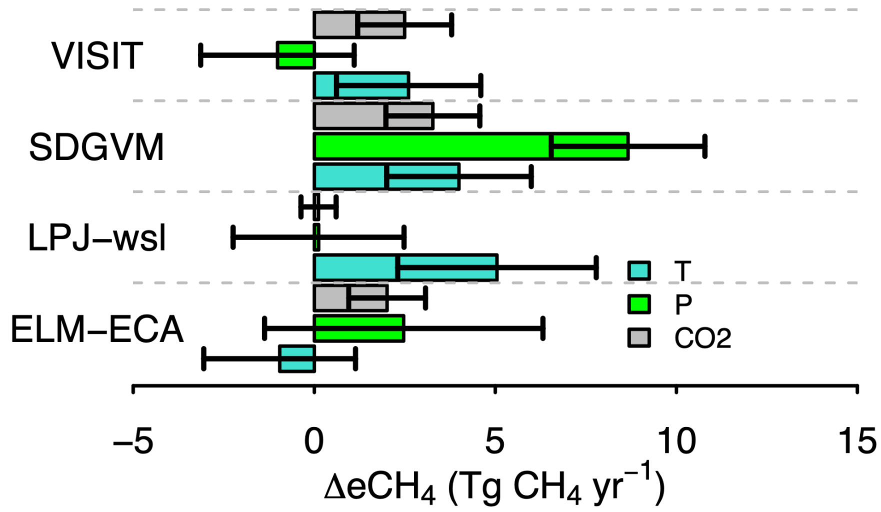


**Figure S6.** Attribution of mean $\Delta eCH_4$ to the temperature (T), precipitation (P), and rising atmospheric $CO_2$ concentration ($CO_2$) based on factorial simulations of a subset of the models.

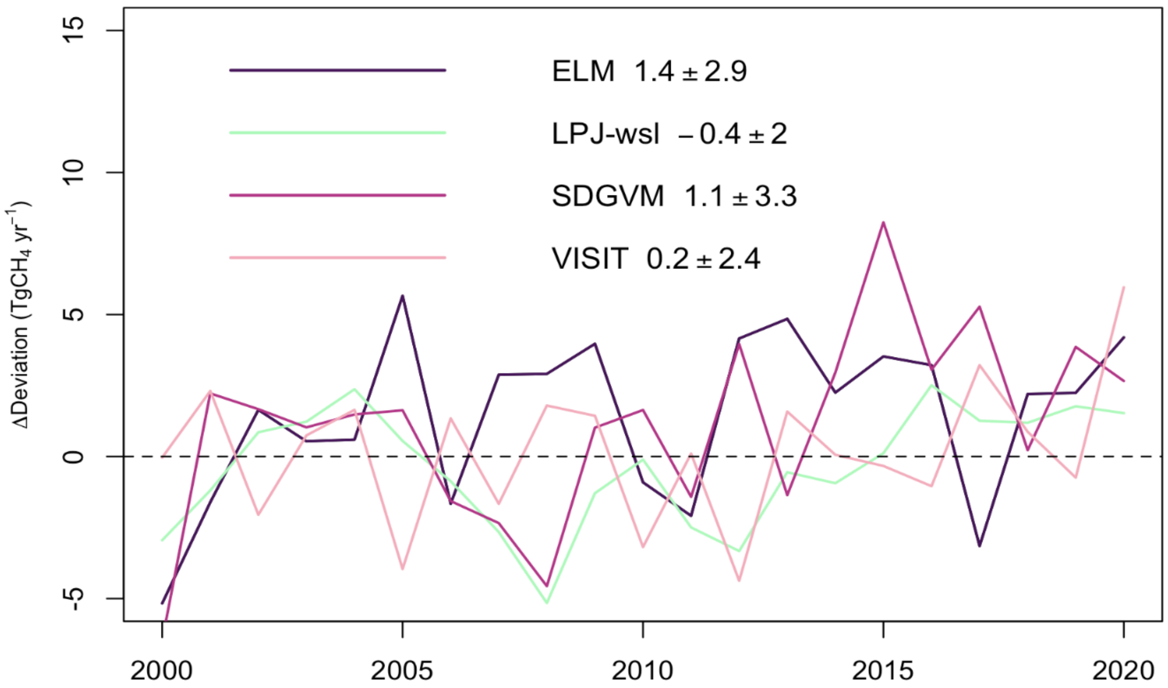


**Figure S7. Time series of differences in $eCH_4$ between the subset of models from the factorial experiments and the annual mean from the full model ensemble.** The mean deviation and one standard deviation are shown in the figure.

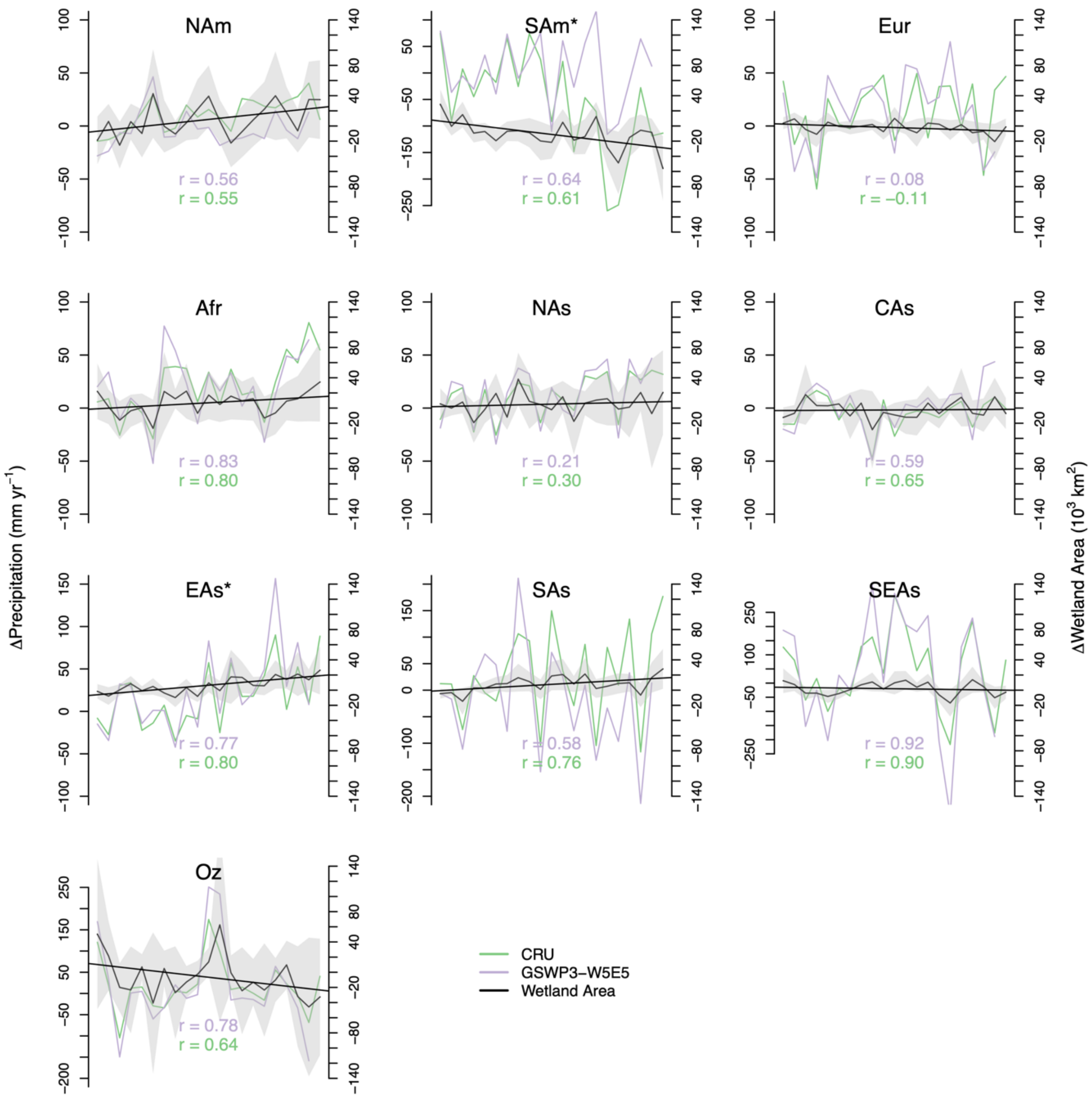
NAm
r = 0.56
r = 0.55
SAm*
r = 0.64
r = 0.61
Eur
r = 0.08
r = −0.11
Afr
r = 0.83
r = 0.80
NAs
r = 0.21
r = 0.30
CAs
r = 0.59
r = 0.65
EAs*
r = 0.77
r = 0.80
SAs
r = 0.58
r = 0.76
SEAs
r = 0.92
r = 0.90
Oz
r = 0.78
r = 0.64
ΔPrecipitation (mm yr$^{-1}$)
ΔWetland Area (10$^3$ km$^2$)
CRU
GSWP3−W5E5
Wetland Area

**Figure S8. Temporal variations of anomaly in precipitation and wetland area relative to the average of 2000-2006 over global wetlands.** The precipitation inputs from CRU and GSWP3-W5E5, along with the ensemble mean of simulated wetland areas (black line) with its 1-σ uncertainty (grey area) derived from eighteen prognostic estimates by the wetland models, are presented. The statistically significant linear regional trends in wetland area are denoted with a star next to the region name. The Spearman correlations between precipitation and wetland area across regions are indicated in color corresponding to different precipitation inputs. The wetland mask is defined by maximum areal extent of the wetland product WAD2M. Region Abbreviations: NAm, North America; SAm, South America; Eur, Europe; Afr, Africa; NAs, North Asia; CAs, Central Asia, EAs, East Asia; Sas, South Asia; SEAs, Southeast Asia; Oz, Oceania.

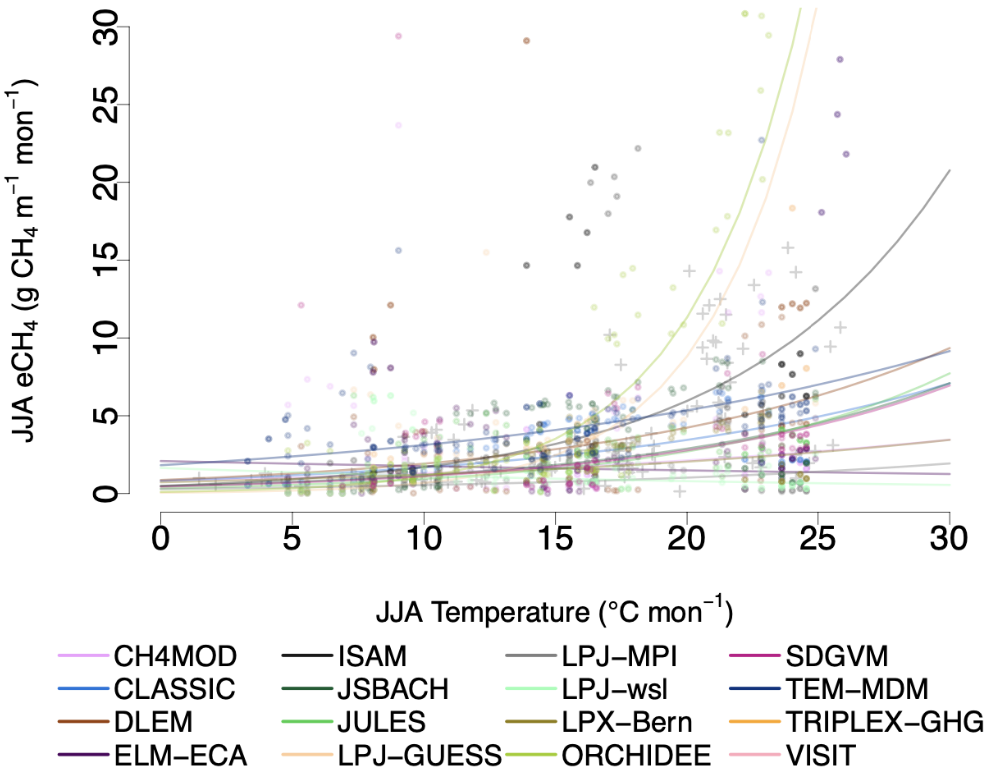


**Figure S9. simulated seasonal eCH$_4$ along geographic temperature gradient across locations of FLUXNET-CH$_4$ sites from individual models for the JJA season.**

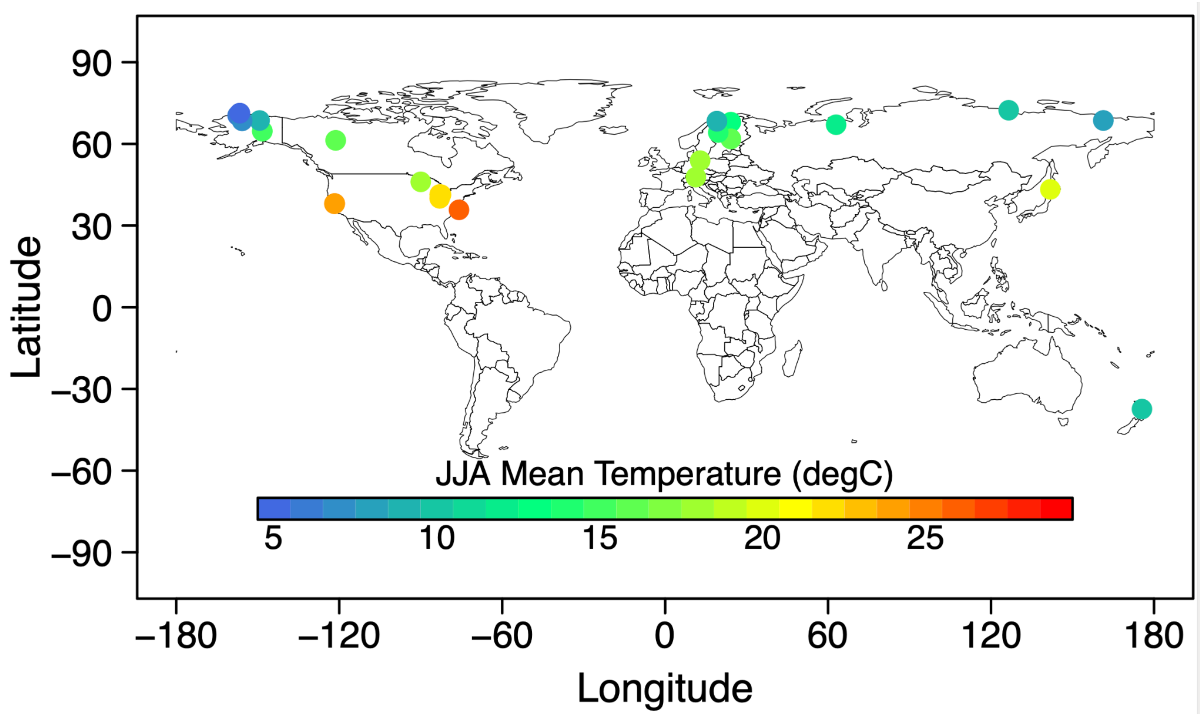


**Figure S10. Map of FLUXNET-$CH_4$ sites applied in the $Q_{10}$ calculation.** The color of the points (n = 34) represents the average JJA temperature for 2000-2020 for each site. The site info can be found at Table S4.

**Tables**

**Table S1. List of GCP-CH4 participating wetland models.** Not all models contributed results to all experiments. The details on the model set-ups and models' methane flux parameterizations can be found in principal references.

| Model | Wetland PFT | Components of $CH_4$ Flux | $CH_4$ Transport Pathway | Temperature Response Functions | $CH_4$ Production Proxy | Nitrogen Cycles | Fire | Spatial Resolution (deg) | Forcing Time Step | Reference |
|---|---|---|---|---|---|---|---|---|---|---|
| $CH4MOD_{wetland}$ | Herbaceous wetland PFTs and Woody wetland | Net flux | Ebullition and Diffusion, and Plant mediated transport | Layered soil temperature | Carbon Substrate | No | No | 0.5 | Monthly | Li et al., 2020 |

| | | | | | | | | | | |
|---|---|---|---|---|---|---|---|---|---|---|
| | PFTs | | | | | | | | | |
| CLASSIC | No wetland-specific PFTs | Net flux | No specific transport pathways | Indirectly through Rh (see Section A3.2 in Melton and Arora 2016 | Rh is scaled to account for $CH_4$ vs. $CO_2$ emitted and differences in upland vs. lowland Rh | No | Yes | T63 (~2.8) | 30 minutes | Arora et al., 2018 |
| DLEM | Generic wetland PFTs | gross production; gross consumption; oxidation; | No specific transport pathways | Layered soil temperature | Carbon Substrate | Yes | No | 0.5 | Daily | Tian, 2015; Tian et al., 2016 |
| ELM-ECA | No wetland-specific PFTs | gross production; gross consumption; oxidation; diffusive, aerenchyma, and ebullition fluxes | Ebullition and Diffusion, and Plant mediated transport | Q10 based on soil T in each soil layer | Rh in each soil layer is scaled to estimate CH4 production | Yes | Yes | ~2° | 6-Hourly | Zhu et al., 2016;2019 |
| ISAM | Upland PFTs, generic wetland PFTs, and Woody wetland PFTs | gross production, oxidation, | Ebullition and Diffusion | | Heterotrophic respiration | Yes | No | 0.5 | 6-Hourly | Shu 2020. Xu 2021. |
| JSBACH | Generic wetland PFT with C3 grass parameters for vegetation | gross production, oxidation | Ebullition and Diffusion, and Plant mediated transport | Layered soil temperature, different temperature responses for production, consumption | CH4 production depends on anoxic respiration produced by YASSO soil carbon model modified to account for anoxic conditions and coupled to JSBACH | No | No | 1.875° | Daily | Kleinen et al., 2020; 2021. |
| JULES | No wetland-specific PFTs | Net fluxes | No specific transport pathways | Layered soil temperature | Net Primary Production | No | No | 0.5 | Daily | Clark 2011. Gedney 2019 |
| LPJ-MPI | Upland PFTs, non-vascular PFTs, Hebaceous wetland PFTs | gross production and oxidation | Ebullition and Diffusion, and Plant mediated transport | Layered soil temperature, different temperature responses for production, consumption, diffusion | Heterotrophic respiration | No | Yes | 0.5 | Monthly | Kleinen et al., 2012 |
| LPJ-wsl | No wetland-specific PFTs | net flux | No specific transport pathways | Soil temperature calculation in LPJ is 12 layers scheme following Wania et al., (2009). Daily average soil temperature for 0-50 cm depth is used for CH4 function. | Heterotrophic respiration | No | Yes | 0.5 | Monthly | Zhang et al., 2016, 2018 |
| LPJ-GUESS | High-latitude (> 40°N): Wetland grass, cushion forbs, lichens, sphagnum moss. South of 40°N: C3 and C4 grasses only on wetlands | Net and gross emissions are simulated for high-latitude (> 40°N) ecosystems. South of 40°N: net emissions only based on a simple rescaling of heterotrophic respiration. | Diffusion, plant-mediated, and ebullition pathways for > 40N | Decomposition of litter and SOM uses an empirical relationship for temperature response of soil temperature at 25 cm depth (calculated following Wania et al., (2009a)) across ecosystems, incorporating damping of Q10 response due to temperature acclimation. $CH_4$ | $CH_4$ production depends on soil temperature in each 10 cm soil layer, the degree of anoxia and the availability of substrate that consists of a fraction of litter and | Yes | No, not on wetlands | 0.5 | Monthly, interpolated to quasi-daily values | McGuire et al., 2012; Wania et al., 2010 |

| | | | | | | | | | | |
|---|---|---|---|---|---|---|---|---|---|---|
| | | | | production, oxidation and transport use temperature dependencies from Wania et al. (2010), from each 10cm layer in the soil. | soil carbon decomposition | | | | | |
| LPX-Bern | wetland PFTs include non-vascular, Herbaceous wetland, and Woody wetland PFTs | gross production; gross consumption; net flux | Ebullition and Diffusion, and Plant mediated transport | Layered soil temperature, different temperature responses for production, consumption, diffusion | Heterotrophic respiration and carbon substrate | Yes | Yes | 0.5 | Monthly | Spahni et al., 2011; Stocker et al., 2014 |
| ORCHIDEE | No wetland-specific PFTs | gross emission (gross production and oxidation) are simulated | Ebullition and Diffusion, and Plant mediated transport | Microbial activities are not represented directly. Only soil temperature and soil moisture which influence microbial activities are considered | Carbon Substrate | No | No | 1 | Daily | Ringeval et al., 2012; Guimberteau 2018 |
| SDGVM | upland PFTs | Net flux | No specific transport pathways | Q10 coefficient using air temperature | Heterotrophic respiration | Yes | Yes | 0.5 | Monthly | SDGVM: Beerling & Woodward 2001;Fluxes following: Singarayer et al., 2011; Wetland area foloowing: Hopcroft et al., 2020 |
| TEM-MDM | Five primary types of wetlands are considered in boreal, temperate and tropical regions (total 15 subtypes). They are forested bog, nonforested bog, forested swamp, nonforested swamp and alluvial formations | gross production; gross consumption; net flux | Ebullition and Diffusion, and Plant mediated transport | Q10 coefficient is used to account for soil temperature effects on methanotrophy rates within each 1 cm layer of the soil profile | $CH_4$ production is modeled as an anaerobic process that occurs in the saturated zone of the soil profile, controlled by methanogenic substrate availability, soil temperatures, PH, and redox potential. | Yes | No | 0.5 | Daily | Zhuang et al., 2004; Liu et al., 2020 |
| VISIT | No wetland-specific PFTs | gross production; gross consumption; net flux; | Ebullition and Diffusion, and Plant mediated transport | Layered soil temperature. | Net Primary Production | No | Yes | 0.5 | Monthly | Ito and Inatomi, 2012; Ito et al., 2019 |
| TRIPLEX-GHG | a general wetland PFT was added without considering | net flux | Ebullition and Diffusion, and Plant mediated transport | Soil temperature factor was evaluated with and exponential function that considering soil temperature and optimum soil | $CH_4$ production was calculated as a proportion of heterotrophic | Yes | No | 0.5 | Daily | (Zhu et al., 2015, 2017) |

| | | | | | | | | | | |
|---|---|---|---|---|---|---|---|---|---|---|
| | specific wetland plants type | | | temperature for $CH_4$ production. The Q10 in the temperature function for $CH_4$ production and $CH_4$ oxidation could be calibrated separately. | respiration ($CO_2$–C) along with soil temperature, Eh and pH modification factors | | | | | |

**Table S2. Factorial simulation setup for 2007-2020.**

| Simulation | Temperature | Precipitation | $CO_2$ concentration |
|---|---|---|---|
| Transient | varying | varying | varying |
| Baseline | climatology of 2000-2006 | climatology of 2000-2006 | 2006 value |
| Temperature Fix run | climatology of 2000-2006 | varying | varying |
| Precipitation Fix run | varying | climatology of 2000-2006 | varying |
| $CO_2$ concentration Fix run | varying | varying | 2006 value |

**Table S3. Modeled $CH_4$ emissions (Unit: $TgCH_4\ yr^{-1}$) and comparison with estimates from bottom-up (BU) and top-down (TD) studies for regional $CH_4$ hotspots.**

| Region | Emissions ($TgCH_4\ yr^{-1}$) | Method | Reference |
|---|---|---|---|
| Amazon | 24±11 | BU modeling | This study |
| | 29 | BU upscaling | Melack et al., 2004 |
| | 47.3-53.0 | TD inversion* | Bergamaschi et al., 2009 |
| | 44±4.8 | TD inversion* | Ringeval et al., 2014 |
| | 31.0-42.0 | TD inversion* | Wilson et al., 2016 |
| | 35±5.6-41.7±5.9 | BU upscaling* | Pangala et al., 2017 |
| | 38.2±5.3-45.6±5.2 | TD inversion* | Wilson et al., 2021 |
| | 33.8±10.9 | TD inversion* | Basso et al., 2021 |
| | 9.2±1.8 | TD inversion | Tunnicliffe et al., 2020 |
| | 39.4±10.3 | BU modeling | Bloom et al., 2017 |
| HBL | 3±2.1 | BU modeling | This study |
| | 2.3 | TD inversion | Pickett-Heaps et al., 2011 |
| WSL | 4.7±2.9 | BU modeling | This study |
| | 6.1±1.2 | TD inversion | Bohn et al., 2015 |
| | 5.3±0.5 | BU modeling | Melton et al., 2013 |
| | 3.9±1.3 | BU upscaling | Glagolev et al., 2011 |
| Alaska | 1.0±0.65 | BU modeling | This study |
| | 2.1±0.5 | TD inversion | Chang et al., 2014 |
| | 1.7±0.3 | TD inversion | Miller et al., 2016 |
| Pantanal | 1.3±0.94 | BU modeling | This study |
| | 3.3 | BU upscaling | Marani and Alvalá, 2007 |
| | 2.1-3.6 | BU modeling | Gerlein-Safdi et al., 2021 |
| | 2.0-2.8 or 3.3 | TD inversion | Gloor et al., 2021 |

| | | | |
|---|---|---|---|
| Sudd | 1.1±1.9 | BU modeling | This study |
| | 1.1±0.5 | BU modeling | Bloom et al., 2017 |
| | 2.5-7** | TD inversion | Lunt et al., 2019 |
| | 7.2±3.2** | TD inversion | Pandey et al., 2021 |
| | 2.1-3.6** | BU modeling | Gerlein-Safdi et al., 2021 |

* These numbers do not distinguish generic wetland applied in this study with the estimates from open water system (e.g., rivers, lakes, ponds, and reservoirs)

**These numbers are derived from a short time period (2017-2020) when the strong positive anomaly occurred at Sudd wetlands, while the model ensemble is average of 2000-2020 level.

**Table S4. FLUXNET-$CH_4$ site used in the temperature dependence analysis.**

| Site ID | Site Name | Country | LAT | LON | Biome | Ecosystem Type | Site PIs | DOI/ Dataset |
|---|---|---|---|---|---|---|---|---|
| CA-Scb | Scotty Creek Bog | Canada | 61.31 | -121.30 | Boreal Forests | Bog | Oliver Sonnentag | AmeriFlux |
| CA-Scc | Scotty Creek Peat plateau/collapse scar | Canada | 61.31 | -121.30 | Boreal Forests | Peat plateau | Oliver Sonnentag | doi:10.17190/A MF/1480303 |
| DE-Sfn | Schechenfilz Nord | Germany | 47.81 | 11.33 | Temperate | Bog | Hans Peter Schmid | European Fluxes Database Cluster |
| DE-Zrk | Zarnekow | Germany | 53.88 | 12.89 | Temperate | Fen | Torsten Sachs | European Fluxes Database Cluster |
| FI-Lom | Lompolojankka | Finland | 68.00 | 24.21 | Boreal Forests | Fen | Annalea Lohila, Mika Aurela | European Fluxes Database Cluster |
| FI-Si2 | Siikaneva II | Finland | 61.84 | 24.17 | Boreal Forests | Bog | Timo Vesala & Ivan Mammarella | European Fluxes Database Cluster |
| FI-Sii | Siikaneva I | Finland | 61.83 | 24.19 | Boreal Forests | Fen | Timo Vesala & Ivan Mammarella | European Fluxes Database Cluster |
| JP-Bby | Bibai Mire | Japan | 43.32 | 141.81 | Temperate | Bog | Masahito Ueyama | European Fluxes Database Cluster |
| NZ-Kop | Kopuatai | New Zealand | -37.39 | 175.55 | Temperate | Bog | Dave Campbell | https://researchc ommons.waikato.ac.nz/handle/10 289/11393 |
| RU-Ch2 | Chersky reference | Russia | 68.62 | 161.35 | Boreal Forests | Wet tundra | Matthias Goeckede | European Fluxes Database Cluster |
| RU-Che | Chersky | Russia | 68.61 | 161.34 | Boreal Forests | Wet tundra | Matthias Goeckede | European Fluxes Database Cluster |
| RU-Sam | Samoylov | Russia | 72.37 | 126.50 | Tundra | Wet tundra | Torsten Sachs | European Fluxes Database Cluster |
| RU-Vrk | Seida/Vorkuta | Russia | 67.06 | 62.94 | Tundra | Wet tundra | Thomas Friborg | European Fluxes Database Cluster |
| SE-Deg | Degero | Sweden | 64.18 | 19.56 | Boreal Forests | Fen | Mats Nilsson | European Fluxes Database Cluster |
| SE-St1 | Stordalen grassland (Mire) | Sweden | 68.35 | 19.05 | Tundra | Fen | Thomas Friborg | European Fluxes Database Cluster |
| SE-Sto | Stordalen Palsa Bog | Sweden | 68.36 | 19.05 | Tundra | Bog | Thomas Friborg | European Fluxes Database Cluster |
| US-Atq | Atqasuk | USA | 70.47 | -157.41 | Tundra | Wet tundra | Donatella Zona | doi:10.17190/A MF/1246029 |
| US-Beo | Barrow | USA | 71.28 | -156.61 | Tundra | Wet tundra | Donatella Zona | AmeriFlux |
| US-Bes | Barrow | USA | 71.28 | -156.6 | Tundra | Wet tundra | Donatella Zona | AmeriFlux |
| US-Bgl | Bog Lake peatland | USA | 47.53 | -93.74 | Temperate | Fen | Narasinha Shurpali | AmeriFlux |
| US-Bzb | Thermokarst collapse bog | USA | 64.70 | -148.32 | Boreal Forests | Bog | Eugenie Euskirchen | AmeriFlux |
| US-Bzf | Rich Fen | USA | 64.70 | -148.31 | Boreal Forests | Fen | Eugenie Euskirchen | AmeriFlux |

| | | | | | | | | |
|---|---|---|---|---|---|---|---|---|
| US-Ics | Wet sedge tundra | USA | 68.61 | -149.31 | Tundra | Wet tundra | Eugenie Euskirchen | doi: 10.17190/AM F/1246130 |
| US-Ivo | Ivotuk | USA | 68.49 | -155.75 | Tundra | Wet tundra | Donatella Zona | doi:10.17190/A MF/1246067 |
| US-Los | Lost Creek | USA | 46.08 | -89.98 | Temperate | Fen | Ankur Desai | doi: 10.17190/AM F/1246071 |
| US-Myb | Mayberry Wetland | USA | 38.05 | -121.77 | Temperate | Marsh | Dennis Baldocchi | doi: 10.17190/AM F/1246139 |
| US-NC4 | NC Alligator River | USA | 35.79 | -75.90 | Temperate | Swamp | Asko Noormets | doi:10.17190/A MF/1480314 |
| US-Ngb | NGEE Barrow | USA | 71.28 | -156.61 | Tundra | Wet tundra | Margaret Torn | doi: 10.17190/AM F/1436326 |
| US-ORv | River Wetland Research Park | USA | 40.02 | -83.02 | Temperate | Marsh | Gil Bohrer | doi:10.17190/A MF/1246135 |
| US-Owc | Old Woman Creek | USA | 41.38 | -82.51 | Temperate | Marsh | Gil Bohrer | doi: 10.17190/AM F/1246094 |
| US-Sne | Sherman Island Restored Wetland | USA | 38.04 | -121.76 | Temperate | Marsh | Dennis Baldocchi | doi: 10.17190/AM F/1418684 |
| US-Tw1 | Twitchell West Pond Wetland | USA | 38.11 | -121.65 | Temperate | Marsh | Dennis Baldocchi | doi: 10.17190/AM F/1246147 |
| US-Tw4 | Twitchell East End Wetland | USA | 38.10 | -121.64 | Temperate | Marsh | Dennis Baldocchi | doi: 10.17190/AM F/1246148 |
| US-Wpt | Winous Point North Marsh | USA | 41.46 | -83.00 | Temperate | Marsh | Housen Chu | doi: 10.17190/AM F/1246155 |

## References

Arora, V. K., Melton, J. R., and Plummer, D.: An assessment of natural methane fluxes simulated by the CLASS-CTEM model, Biogeosciences, 15, 4683–4709, https://doi.org/10.5194/bg-15-4683-2018, 2018.

Basso, L. S., Marani, L., Gatti, L. V., Miller, J. B., Gloor, M., Melack, J., Cassol, H. L. G., Tejada, G., Domingues, L. G., Arai, E., Sanchez, A. H., Corrêa, S. M., Anderson, L., Aragão, L. E. O. C., Correia, C. S. C., Crispim, S. P., and Neves, R. A. L.: Amazon methane budget derived from multi-year airborne observations highlights regional variations in emissions, Commun Earth Environ, 2, 1–13, https://doi.org/10.1038/s43247-021-00314-4, 2021.

Bloom, A. A., Bowman, K. W., Lee, M., Turner, A. J., Schroeder, R., Worden, J. R., Weidner, R., McDonald, K. C., and Jacob, D. J.: A global wetland methane emissions and uncertainty dataset for atmospheric chemical transport models (WetCHARTs version 1.0), Geoscientific Model Development, 10, 2141–2156, https://doi.org/10.5194/gmd-10-2141-2017, 2017.

Bohn, T. J., Melton, J. R., Ito, A., Kleinen, T., Spahni, R., Stocker, B. D., Zhang, B., Zhu, X., Schroeder, R., Glagolev, M. V., Maksyutov, S., Brovkin, V., Chen, G., Denisov, S. N., Eliseev, A. V., Gallego-Sala, A., McDonald, K. C., Rawlins, M. A., Riley, W. J., Subin, Z. M., Tian, H., Zhuang, Q., and Kaplan, J. O.: WETCHIMP-WSL: intercomparison of wetland methane emissions models over West Siberia, Biogeosciences, 12, 3321–3349, https://doi.org/10.5194/bg-12-3321-2015, 2015.

Chang, R. Y.-W., Miller, C. E., Dinardo, S. J., Karion, A., Sweeney, C., Daube, B. C., Henderson, J. M., Mountain, M. E., Eluszkiewicz, J., Miller, J. B., Bruhwiler, L. M. P., and Wofsy, S. C.: Methane emissions from Alaska in 2012 from CARVE airborne observations, Proceedings of the National Academy of Sciences, 111, 16694–16699, https://doi.org/10.1073/pnas.1412953111, 2014.

Gerlein-Safdi, C., Bloom, A. A., Plant, G., Kort, E. A., and Ruf, C. S.: Improving Representation of Tropical Wetland Methane Emissions With CYGNSS Inundation Maps, Global Biogeochemical Cycles, 35, e2020GB006890, https://doi.org/10.1029/2020GB006890, 2021.

Glagolev, M., Kleptsova, I., Filippov, I., Maksyutov, S., and Machida, T.: Regional methane emission from West Siberia mire landscapes, Environmental Research Letters, 6, 045214, https://doi.org/10.1088/1748-9326/6/4/045214, 2011.

Gloor, M., Gatti, L. V., Wilson, C., Parker, R. J., Boesch, H., Popa, E., Chipperfield, M. P., Poulter, B., Zhang, Z., Basso, L., Miller, J., McNorton, J., Jimenez, C., and Prigent, C.: Large Methane Emissions From the Pantanal During Rising Water-Levels Revealed by Regularly Measured Lower Troposphere CH4 Profiles, Global Biogeochemical Cycles, 35, e2021GB006964, https://doi.org/10.1029/2021GB006964, 2021.

Hopcroft, P. O., Ramstein, G., Pugh, T. A. M., Hunter, S. J., Murguia-Flores, F., Quiquet, A., Sun, Y., Tan, N., and Valdes, P. J.: Polar amplification of Pliocene climate by elevated trace gas radiative forcing, PNAS, 117, 23401–23407, https://doi.org/10.1073/pnas.2002320117, 2020.

Ito, A. and Inatomi, M.: Use of a process-based model for assessing the methane budgets of global terrestrial ecosystems and evaluation of uncertainty, Biogeosciences, 9, 759–773, https://doi.org/10.5194/bg-9-759-2012, 2012.

Ito, A., Tohjima, Y., Saito, T., Umezawa, T., Hajima, T., Hirata, R., Saito, M., and Terao, Y.: Methane budget of East Asia, 1990–2015: A bottom-up evaluation, Science of The Total Environment, https://doi.org/10.1016/j.scitotenv.2019.04.263, 2019.

Kleinen, T., Brovkin, V., and Schuldt, R. J.: A dynamic model of wetland extent and peat accumulation: results for the Holocene, Biogeosciences, 9, 235–248, https://doi.org/10.5194/bg-9-235-2012, 2012.

Li, T., Lu, Y., Yu, L., Sun, W., Zhang, Q., Zhang, W., Wang, G., Qin, Z., Yu, L., Li, H., and Zhang, R.: Evaluation of CH4MODwetland and Terrestrial Ecosystem Model (TEM) used to estimate global CH4 emissions from natural wetlands, Geosci. Model Dev., 13, 3769–3788, https://doi.org/10.5194/gmd-13-3769-2020, 2020.

Liu, L., Zhuang, Q., Oh, Y., Shurpali, N. J., Kim, S., and Poulter, B.: Uncertainty Quantification of Global Net Methane Emissions From Terrestrial Ecosystems Using a Mechanistically Based Biogeochemistry Model, Journal of Geophysical Research: Biogeosciences, 125, e2019JG005428, https://doi.org/10.1029/2019JG005428, 2020.

Lunt, M. F., Palmer, P. I., Feng, L., Taylor, C. M., Boesch, H., and Parker, R. J.: An increase in methane emissions from tropical Africa between 2010 and 2016 inferred from satellite data, Atmospheric Chemistry and Physics, 19, 14721–14740, https://doi.org/10.5194/acp-19-14721-2019, 2019.

Marani, L. and Alvalá, P. C.: Methane emissions from lakes and floodplains in Pantanal, Brazil, Atmospheric Environment, 41, 1627–1633, https://doi.org/10.1016/j.atmosenv.2006.10.046, 2007.

McGuire, A. D., Christensen, T. R., Hayes, D., Heroult, A., Euskirchen, E., Kimball, J. S., Koven, C., Lafleur, P., Miller, P. A., Oechel, W., Peylin, P., Williams, M., and Yi, Y.: An assessment of the carbon balance of Arctic tundra: comparisons among observations, process models, and atmospheric inversions, Biogeosciences, 9, 3185–3204, https://doi.org/10.5194/bg-9-3185-2012, 2012.

Melack, J. M., Hess, L. L., Gastil, M., Forsberg, B. R., Hamilton, S. K., Lima, I. B. T., and Novo, E. M. L. M.: Regionalization of methane emissions in the Amazon Basin with microwave remote sensing, Global Change Biology, 10, 530–544, https://doi.org/10.1111/j.1365-2486.2004.00763.x, 2004.

Melton, J. R., Wania, R., Hodson, E. L., Poulter, B., Ringeval, B., Spahni, R., Bohn, T., Avis, C. A., Beerling, D. J., Chen, G., Eliseev, A. V., Denisov, S. N., Hopcroft, P. O., Lettenmaier, D. P., Riley, W. J., Singarayer, J. S., Subin, Z. M., Tian, H., Zürcher, S., Brovkin, V., van Bodegom, P. M., Kleinen, T., Yu, Z. C., and Kaplan, J. O.: Present state of global wetland extent and wetland methane modelling: conclusions from a model inter-comparison project (WETCHIMP), Biogeosciences, 10, 753–788, https://doi.org/10.5194/bg-10-753-2013, 2013.

Miller, S. M., Miller, C. E., Commane, R., Chang, R. Y.-W., Dinardo, S. J., Henderson, J. M., Karion, A., Lindaas, J., Melton, J. R., Miller, J. B., Sweeney, C., Wofsy, S. C., and Michalak, A. M.: A multiyear estimate of methane fluxes in Alaska from CARVE atmospheric observations: METHANE FLUXES FROM ALASKA, Global Biogeochemical Cycles, 30, 1441–1453, https://doi.org/10.1002/2016GB005419, 2016.

Pandey, S., Houweling, S., Lorente, A., Borsdorff, T., Tsivlidou, M., Bloom, A. A., Poulter, B., Zhang, Z., and Aben, I.: Using satellite data to identify the methane emission controls of South Sudan's wetlands, Biogeosciences, 18, 557–572, https://doi.org/10.5194/bg-18-557-2021, 2021.

Pangala, S. R., Enrich-Prast, A., Basso, L. S., Peixoto, R. B., Bastviken, D., Hornibrook, E. R. C., Gatti, L. V., Marotta, H., Calazans, L. S. B., Sakuragui, C. M., Bastos, W. R., Malm, O., Gloor, E., Miller, J. B., and Gauci, V.: Large emissions from floodplain trees close the Amazon methane budget, Nature, 552, 230–234, https://doi.org/10.1038/nature24639, 2017.

Pickett-Heaps, C. A., Jacob, D. J., Wecht, K. J., Kort, E. A., Wofsy, S. C., Diskin, G. S., Worthy, D. E. J., Kaplan, J. O., Bey, I., and Drevet, J.: Magnitude and seasonality of wetland methane emissions from the Hudson Bay Lowlands (Canada), Atmospheric Chemistry and Physics, 11, 3773–3779, https://doi.org/10.5194/acp-11-3773-2011, 2011.

Ringeval, B., Decharme, B., Piao, S. L., Ciais, P., Papa, F., de Noblet-Ducoudré, N., Prigent, C., Friedlingstein, P., Gouttevin, I., Koven, C., and Ducharne, A.: Modelling sub-grid wetland in the ORCHIDEE global land surface model: evaluation against river discharges and remotely sensed data, Geoscientific Model Development, 5, 941–962, https://doi.org/10.5194/gmd-5-941-2012, 2012.

Ringeval, B., Houweling, S., van Bodegom, P. M., Spahni, R., van Beek, R., Joos, F., and Röckmann, T.: Methane emissions from floodplains in the Amazon Basin: challenges in developing a process-based model for global applications, Biogeosciences, 11, 1519–1558, https://doi.org/10.5194/bg-11-1519-2014, 2014.

Singarayer, J. S., Valdes, P. J., Friedlingstein, P., Nelson, S., and Beerling, D. J.: Late Holocene methane rise caused by orbitally controlled increase in tropical sources, Nature, 470, 82–85, https://doi.org/10.1038/nature09739, 2011.

Spahni, R., Wania, R., Neef, L., van Weele, M., Pison, I., Bousquet, P., Frankenberg, C., Foster, P. N., Joos, F., Prentice, I. C., and van Velthoven, P.: Constraining global methane emissions and uptake by ecosystems, Biogeosciences, 8, 1643–1665, https://doi.org/10.5194/bg-8-1643-2011, 2011.

Stocker, B. D., Spahni, R., and Joos, F.: DYPTOP: a cost-efficient TOPMODEL implementation to simulate sub-grid spatio-temporal dynamics of global wetlands and peatlands, Geoscientific Model Development Discussions, 7, 4875–4930, https://doi.org/10.5194/gmdd-7-4875-2014, 2014.

Tian, B.: Spread of model climate sensitivity linked to double-Intertropical Convergence Zone bias, Geophysical Research Letters, 42, 4133–4141, https://doi.org/10.1002/2015GL064119, 2015.

Tian, H., Lu, C., Ciais, P., Michalak, A. M., Canadell, J. G., Saikawa, E., Huntzinger, D. N., Gurney, K. R., Sitch, S., Zhang, B., Yang, J., Bousquet, P., Bruhwiler, L., Chen, G., Dlugokencky, E., Friedlingstein, P., Melillo, J., Pan, S., Poulter, B., Prinn, R., Saunois, M., Schwalm, C. R., and Wofsy, S. C.: The terrestrial biosphere as a net source of greenhouse gases to the atmosphere, Nature, 531, 225–228, https://doi.org/10.1038/nature16946, 2016.

Tunnicliffe, R. L., Ganesan, A. L., Parker, R. J., Boesch, H., Gedney, N., Poulter, B., Zhang, Z., Lavrič, J. V., Walter, D., Rigby, M., Henne, S., Young, D., and O'Doherty, S.: Quantifying sources of Brazil's CH4 emissions between 2010 and 2018 from satellite data, Atmos. Chem. Phys., 20, 13041–13067, https://doi.org/10.5194/acp-20-13041-2020, 2020.

Wania, R., Ross, I., and Prentice, I. C.: Implementation and evaluation of a new methane model within a dynamic global vegetation model: LPJ-WHyMe v1.3.1, Geoscientific Model Development, 3, 565–584, https://doi.org/10.5194/gmd-3-565-2010, 2010.

Wilson, C., Chipperfield, M. P., Gloor, M., Parker, R. J., Boesch, H., McNorton, J., Gatti, L. V., Miller, J. B., Basso, L. S., and Monks, S. A.: Large and increasing methane emissions from eastern Amazonia derived from satellite data, 2010–2018, Atmospheric Chemistry and Physics, 21, 10643–10669, https://doi.org/10.5194/acp-21-10643-2021, 2021.

Wilson, D., Farrell, C. A., Fallon, D., Moser, G., Müller, C., and Renou-Wilson, F.: Multiyear greenhouse gas balances at a rewetted temperate peatland, Global Change Biology, 22, 4080–4095, https://doi.org/10.1111/gcb.13325, 2016.

Zhang, Z., Zimmermann, N. E., Kaplan, J. O., and Poulter, B.: Modeling spatiotemporal dynamics of global wetlands: comprehensive evaluation of a new sub-grid TOPMODEL parameterization and uncertainties, Biogeosciences, 13, 1387–1408, https://doi.org/10.5194/bg-13-1387-2016, 2016.

Zhang, Z., Zimmermann, N. E., Calle, L., Hurtt, G., Chatterjee, A., and Poulter, B.: Enhanced response of global wetland methane emissions to the 2015–2016 El Niño-Southern Oscillation event, Environmental Research Letters, 13, 074009, https://doi.org/10.1088/1748-9326/aac939, 2018.

Zhu, Q., Peng, C., Chen, H., Fang, X., Liu, J., Jiang, H., Yang, Y., and Yang, G.: Estimating global natural wetland methane emissions using process modelling: spatio-temporal patterns and contributions to atmospheric methane fluctuations: Global natural wetland methane emissions, Global Ecology and Biogeography, 24, 959–972, https://doi.org/10.1111/geb.12307, 2015.

Zhu, Q., Iversen, C. M., Riley, W. J., Slette, I. J., and Vander Stel, H. M.: Root traits explain observed tundra vegetation nitrogen uptake patterns: Implications for trait-based land models: Tundra N Uptake Model-Data Comparison, Journal of Geophysical Research: Biogeosciences, 121, 3101–3112, https://doi.org/10.1002/2016JG003554, 2016.

Zhu, Q., Peng, C., Ciais, P., Jiang, H., Liu, J., Bousquet, P., Li, S., Chang, J., Fang, X., Zhou, X., Chen, H., Liu, S., Lin, G., Gong, P., Wang, M., Wang, H., Xiang, W., and Chen, J.: Interannual variation in methane emissions from tropical wetlands triggered by repeated El Niño Southern Oscillation, Global Change Biology, 23, 4706–4716, https://doi.org/10.1111/gcb.13726, 2017.

Zhuang, Q., Melillo, J. M., Kicklighter, D. W., Prinn, R. G., McGuire, A. D., Steudler, P. A., Felzer, B. S., and Hu, S.: Methane fluxes between terrestrial ecosystems and the atmosphere at northern high latitudes during the past century: A retrospective analysis with a process-based biogeochemistry model, Global Biogeochemical Cycles, 18, https://doi.org/10.1029/2004GB002239, 2004.